

# Hydrogen wall and heliosheath Ly-alpha absorption toward nearby stars: possible constraints on the heliospheric interface plasma flow

Vlad Izmodenov\*, Brain Wood<sup>†</sup> and Rosine Lallement\*\*

\**Lomonosov Moscow State University, Department of Aeromechanics, Faculty of mechanics and mathematics, Vorob'evy gory, Glavnoe Zdanie MGU, 119899, Moscow, Russia*

<sup>†</sup>*JILA, University of Colorado, and NIST, Boulder, USA*

\*\**Service d'Aeronomie, CNRS, France*

**Abstract.** A self-consistent model of the solar wind interaction with the two-component (plasma and H atoms) interstellar medium is employed to calculate heliospheric Lyman-alpha absorption spectra. It is shown that the heliospheric absorption consists of absorption in the hydrogen wall region and in the heliosheath. Both absorption components are computed in different directions. We perform a parametric study by varying the proton and H atom number densities of the interstellar gas. The theoretical absorption spectra are compared with Hubble Space Telescope observations toward six nearby stars. Results of the comparison and possible constraints on the structure of the heliospheric interface are presented and discussed.

## INTRODUCTION

The heliospheric interface is formed by the interaction of the solar wind with the charged component of the interstellar medium (see Figure 1). Interstellar hydrogen atoms are disturbed in the interface by charge exchange with protons. In the heliospheric interface, atoms newly created by charge exchange have the properties of local protons. Since the plasma properties are different in the four regions of the heliospheric interface shown in Figure 1, the H atoms in the heliosphere can be separated into four populations, each having significantly different properties. For example, population 3 consists of the atoms created by charge exchange with relatively hot protons in the region of disturbed interstellar plasma around the heliopause (region 3 in Figure 1).

The Ly- $\alpha$  transition of atomic H is the strongest absorption line in stellar spectra. Thus, the heated and decelerated atomic hydrogen within the heliosphere produces a substantial amount of Ly- $\alpha$  absorption. The absorption was first detected by Linsky and Wood in 1996 [1] in Ly- $\alpha$  absorption spectra of the very nearby star  $\alpha$  Cen taken by the Goddard High Resolution Spectrograph (GHRS) instrument on board the Hubble Space Telescope (HST). Since that time, it has been realized that the absorption can serve as a remote diagnostic of the heliospheric interface, and for stars in general, their “astrospheric” interfaces.

In this study, we use the Baranov-Malama model [2,

3] of the heliospheric interface to model the heliospheric absorption toward directions of six nearby stars. An advantage of our model is the possibility of separation of heliospheric H atoms into four populations, as discussed above. This model advantage allows us to consider separately two types of heliospheric absorption, hydrogen wall absorption (or absorption by population 3) and heliosheath absorption (or absorption by population 4).

We computed the global heliospheric interface structure and distribution of interstellar hydrogen in the interface using the Baranov-Malama model. Our calculations assume the following values for the fully ionized solar wind at 1 AU:  $n_{p,E} = 6.5 \text{ cm}^{-3}$ ,  $V_{p,E} = 450 \text{ km s}^{-1}$ , and  $M_E = 10$ , where  $n_{p,E}$ ,  $V_{p,E}$  and  $M_E$  are the proton number density, solar wind velocity, and Mach number, respectively. For the inflowing partially ionized interstellar gas, we assume a velocity of  $25.6 \text{ km s}^{-1}$  and a temperature of 7000 K. These values are consistent with in situ observations of interstellar helium. Two other input parameters, interstellar proton and H atom number densities, are varied. The values assumed for these parameters for the various models are listed in Table 1. We vary  $n_{p,LIC}$  in the range  $0.1 - 0.2 \text{ cm}^{-3}$ , while  $n_{H,LIC}$  is varied in the range  $0.05 - 0.2 \text{ cm}^{-3}$ .

The Ly- $\alpha$  lines of these six stars observed by HST are shown in Figure 2 (left column). All of the spectra except that of 36 Oph A were taken using the Goddard High Resolution Spectrograph (GHRS) instrument. The 36 Oph A data were obtained by the Space Telescope

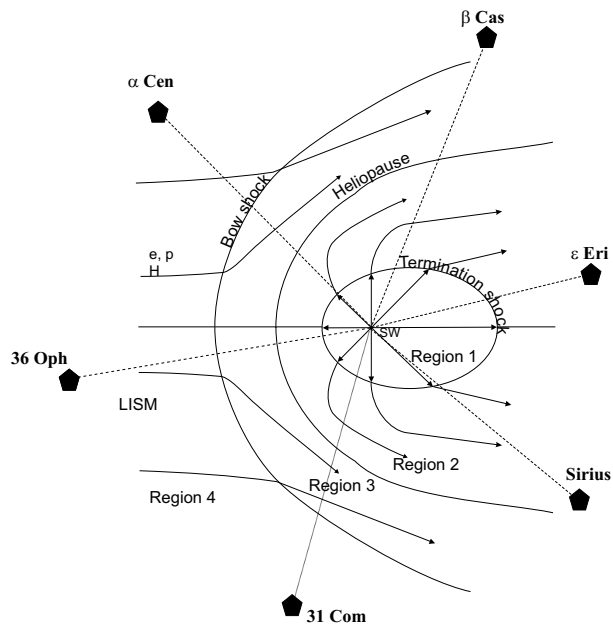


**FIGURE 1.** The heliospheric interface is the region of the solar wind interaction with LIC. The heliopause is a contact discontinuity, which separates the plasma wind from interstellar plasmas. The termination shock decelerates the supersonic solar wind. The bow shock may also exist in the interstellar medium. The heliospheric interface can be divided into four regions with significantly different plasma properties: 1) supersonic solar wind; 2) subsonic solar wind in the region between the heliopause and termination shock (i.e., the heliosheath); 3) disturbed interstellar plasma region (or "pile-up" region) around the heliopause; 4) undisturbed interstellar medium.

Imaging Spectrograph (STIS), which replaced GHRS in 1997. The spectra are plotted on a heliocentric velocity scale. All show broad, saturated H I absorption near line center and narrower deuterium (D I) absorption about  $80 \text{ km s}^{-1}$  blueward of the H I absorption. Figure 2 also shows the assumed intrinsic stellar Ly  $\alpha$  lines and the best estimates for interstellar absorption (e.g., [4] and references therein). Excess absorption on the red side of the Ly  $\alpha$  absorption, when present, is interpreted as heliospheric absorption, while excess absorption on the blue side, when present, is interpreted as astrospheric absorption [Wood *et al.*, 2000]. In this paper we focus on the red side of the Ly  $\alpha$  absorption. The left side of the Ly  $\alpha$  absorption spectra was discussed, for example, in [5, 6]. The stellar profiles and interstellar absorption estimates are based on previously published work, which is summarized in [4].

**TABLE 1.** Sets of model parameters

Model	$n_{H,LIC}$	$n_{p,LIC}$	Notation in figure 2
1	0.10	0.10	solid
2	0.15	0.05	dotted
3	0.15	0.10	dashed
4	0.20	0.05	dot-dash
5	0.20	0.10	dot-dot-dot-dash
6	0.20	0.20	long dash

## COMPARISON OF THEORY AND OBSERVATIONS

The middle and right columns of Figure 2 show the Ly  $\alpha$  lines zoomed in on the red side of the H I absorption line, since that is where most of the heliospheric absorption is expected. The Ly  $\alpha$  profile after interstellar absorption is shown in the plots as solid lines. The middle column also shows Ly  $\alpha$  profiles after interstellar and hydrogen wall absorption, while the right column shows Ly  $\alpha$  profiles after interstellar, hydrogen wall, and heliosheath absorption. The hydrogen wall and heliosheath components are shown for all six models discussed above (see Table 1).

The absorption spectra toward upwind directions (36 Oph and  $\alpha$  Cen) are fitted rather well by hydrogen wall absorption only. In comparing the theoretical absorption with data, the most important place for the model to agree with the data is at the base of the absorption, where it is very difficult (if not impossible) to correct any discrepancies by altering the assumed stellar Ly  $\alpha$  profile [5]. Toward 36 Oph, model 2 produces slightly more absorption and model 6 produces slightly less absorption at its base compared to the data. For other models the differences between model predictions and HST data at the base can be reduced by small corrections to the assumed stellar profile and interstellar absorption. Toward  $\alpha$  Cen, all models show slightly more absorption at the base than the data, except for model 6. It is interesting to note that model 6 fits the  $\alpha$  Cen data remarkably well, while it does not fit as well the Ly  $\alpha$  spectrum of 36 Oph. Note that these discrepancies with the data just discussed are small enough that they could in principle be corrected by reasonably small changes to the assumed stellar Ly  $\alpha$  profile or interstellar absorption, although the better fits in Figure 2 are still to be preferred.

The heliosheath absorption, which is added to the interstellar and hydrogen wall absorption in the right column of Figure 2, does not change the fits much for the upwind lines of sight. Model 2 predicts too much absorption toward both 36 Oph and  $\alpha$  Cen and produces the greatest difference with the data at the base of the absorption where it matters most. Consideration of the heliosheath absorption significantly increases the total heliospheric absorption predicted by model 4. The mod-

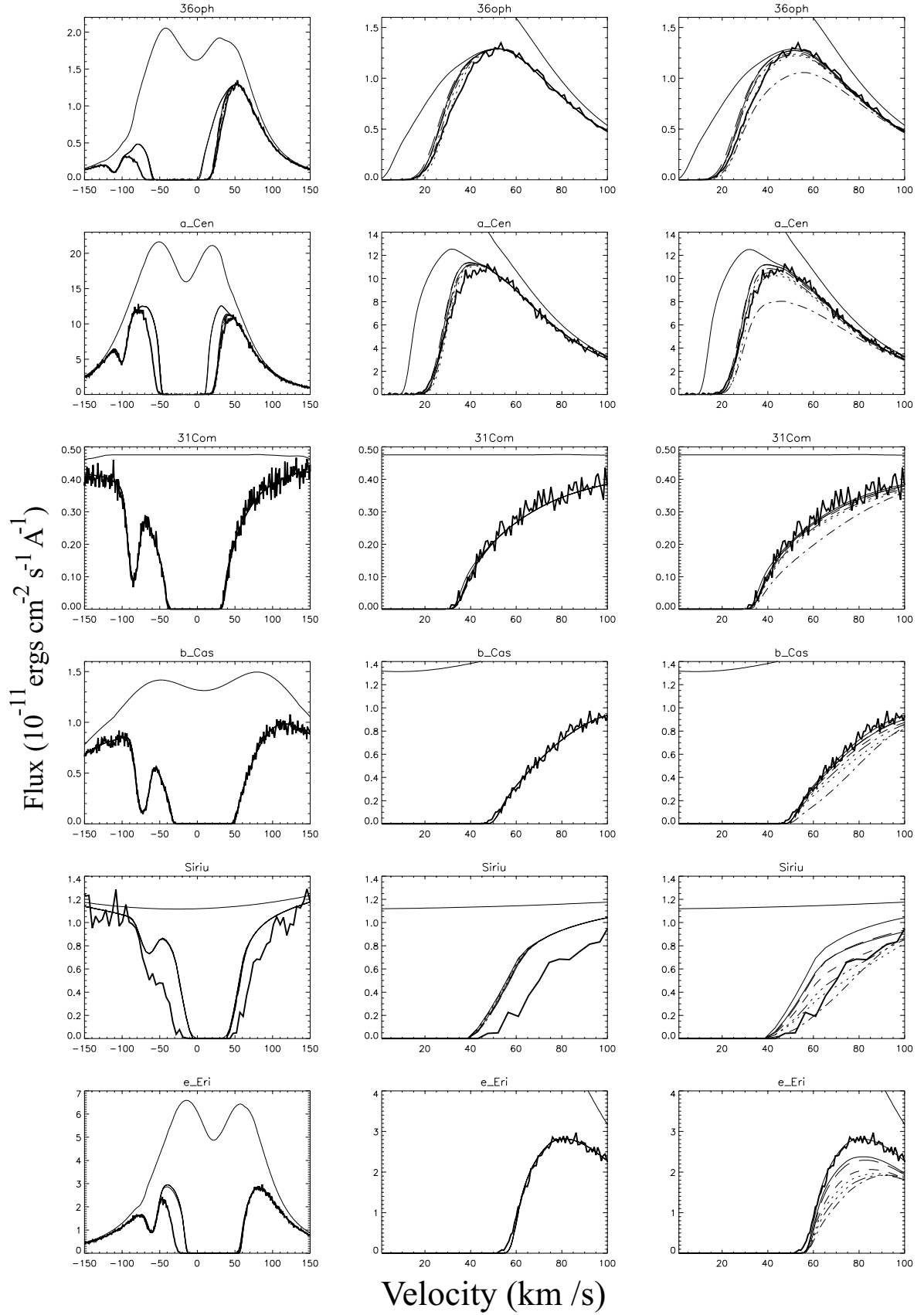


**FIGURE 2.** Left column: HST Ly  $\alpha$  spectra of six stars: 36 Oph,  $\alpha$  Cen, 31 Com,  $\beta$  Cas, Sirius,  $\epsilon$  Eri, respectively from top to bottom. Each plot shows the observed profile (thick solid line), assumed stellar line profile and interstellar absorption (thin solid lines). Middle column: Reproduction of left column, zoomed in on the red side of Ly- $\alpha$  absorption line. In addition, simulated Ly- $\alpha$  profiles after interstellar and hydrogen wall absorption are shown for models 1-6. Solid lines, when it is different from assumed stellar profile and interstellar absorption, correspond to model 1; dotted lines show results of model 2; dashes correspond to model 3; dot-dash curves correspond to model 4, dot-dot-dot-dash lines correspond to model 5, long dashes correspond to model 6. Right column: same as the middle column, but heliosheath absorption is added to the simulated Ly- $\alpha$  profiles.

els with the worst agreement with the upwind directions (model 2 and model 4) correspond to the extreme case of small interstellar proton number density,  $n_{p,LIC}$ .

The observed absorption in the crosswind lines of sight to  $\beta$  Cas shows no need for any heliospheric absorption, and our models do not generally predict significant absorption in the crosswind directions that can be clearly distinguished from interstellar absorption. Significant heliosheath absorption in model 4 makes the model the worst fit to the data in the crosswind directions. The other models fit the data acceptably well.

Results of the comparison for downwind lines of sight are more puzzling. It is clearly seen that the missing absorption toward Sirius can be easily explained by absorption in the heliosheath. Moreover, the heliosheath absorption predicted by different models is noticeably different. Model 4, which has the worst fit to the data for all other lines of sight, fits the observed Sirius spectrum better than other models.

In contrast to Sirius, for  $\epsilon$  Eri the interstellar absorption fits the observed spectrum very well and there is no need for heliospheric absorption. There is no hydrogen wall absorption in this direction (middle column of Figure 2), but all of our models predict too much heliosheath absorption. A similar problem was also found in [5] when they compared their models with the data. The discrepancy may be even more dramatic than our models suggest, because our computational grid extends only 700 AU in the downwind direction, which as stated above is not far enough to account for all the absorption. A larger grid would presumably make the  $\epsilon$  Eri discrepancies worse for all models, and also change which model fits best for Sirius.

## SUMMARY

We have compared H I Ly- $\alpha$  absorption profiles toward six nearby stars observed by HST with theoretical profiles computed using Baranov-Malama model of the heliospheric interface with six different sets of model parameters. Our results are summarized as follows:

1. The absorption produced by the hydrogen wall does not depend significantly on local interstellar H atom and proton number densities for upwind and crosswind directions. In downwind directions the hydrogen wall absorption is sensitive to interstellar densities, but this absorption component is most easily detected in upwind directions. In crosswind and downwind directions the hydrogen wall absorption is hidden in the saturated interstellar absorption and cannot be observed.

2. The heliosheath absorption varies significantly with interstellar proton and H atom number densities. For all models, the heliosheath absorption is more pronounced

in crosswind and downwind directions. The heliosheath absorption is redshifted in crosswind directions compared with the interstellar and hydrogen wall absorption components.

3. Comparison of computations and data shows that all available absorption spectra, except that of Sirius, can be explained by taking into account the hydrogen wall absorption only. Considering heliosheath absorption, we find that all models have a tendency to overpredict heliosheath absorption in downwind directions. Toward upwind and crosswind stars the small differences between model predictions and the data can be corrected by small alterations of the assumed stellar Ly- $\alpha$  profile. However, the downwind  $\epsilon$  Eri line of sight is a problem, as the models predict too much heliosheath absorption in that direction, and for many, if not most, of the models the discrepancy with the data is too great to resolve by reasonable alterations of the stellar profile.

4. It is puzzling that model 4 provides the best fit to the absorption profile toward Sirius but the worst fit to the other lines of sight. This may be due to our models underestimating heliosheath absorption in downwind directions due to limited grid size, or perhaps the detected excess absorption toward Sirius is not really heliospheric in origin, as suggested by other authors [7]. It is also possible that the difficulties the models have with the downwind lines of sight towards Sirius and  $\epsilon$  Eri might be resolved by modifications to the models, perhaps by taking into account the multi-component nature of the heliosheath plasma flow.

## ACKNOWLEDGMENTS

This work was supported in part by INTAS Awards 2001-0270, RFBR grants 01-02-17551, 02-02-06011, 01-01-00759, CRDF Award RP1-2248, and International Space Science Institute in Bern.

## REFERENCES

1. Linsky, J. L., Wood, B. E., *Astrophys. J.*, 463, 254 (1996).
2. Baranov V.B., Malama Yu.G., *J. Geophys. Res.*, 98, 15,157 (1993).
3. Izmodenov, V., Gruntman, M., Malama, Yu. G., *J. Geophys. Res.*, 106, 10681-10690 (2001).
4. Izmodenov, V., Wood, B., Lallement, R., *J. Geophys. Res.*, submitted (2002).
5. Wood, B. E., Müller H. R., G. P. Zank, *Astrophys. J.*, 537, 304-311 (2000).
6. Izmodenov, V. V., Lallement, R., Malama, Yu. G., *Astron. Astrophys.* 342, L13-L16 (1999).
7. Hebrard, G., Mallouris, C., Ferlet, R., Koester, D., Lemoine, M., Vidal-Madjar, A., York, D., *Astron. Astrophys.*, 350, 643 (1999)